Geol Rundsch (1999) 87:633–643

ORIGINAL PAPER

M. Steinmann · P. Stille

Geochemical evidence for the nature of the crust beneath the eastern North Penninic basin of the Mesozoic Tethys ocean

Received: 2 February 1998 / Accepted: 2 November 1998

Abstract The North Penninic basin was a subbasin in the northern part of the Mesozoic Tethys ocean. Its significance within the framework of this ocean is controversial because it is not clear whether it was underlain by thinned continental or oceanic crust. Remnants of the eastern North Penninic basin are preserved in the Alps of eastern Switzerland (Grisons) as low metamorphic "Bündnerschiefer" sediments and associated basaltic rocks which formed approximately 140–170 Ma ago (Misox Bündnerschiefer zone, Middle Jurassic to Early Cretaceous). Nb/U, Zr/Nb, and Y/Nb ratios, as well as Nd–Sr isotopic and REE data of most of the metabasalts point to a depleted MORB-type mantle origin. They have been contaminated by magmatic assimilation of Bündnerschiefer sediments and by exchange with seawater, but do not prove the existence of a subcontinental lithospheric mantle or continental crust beneath the North Penninic basin. This suggests that the studied part of the North Penninic realm was underlain by oceanic crust. Only the metabasalts from two melange zones (Vals and Grava melanges) show a more important contamination by crustal material. Since this type of contamination cannot be observed in the other tectonic units, we suggest that its occurrence is related to melange formation during the subduction of the North Penninic basin in the Tertiary. The North Penninic basin was probably, despite the occurrence of oceanic crust, smaller than the South Penninic ocean where the presence of oceanic crust is well established. Modern analogues for the North Penninic basin could be the transitional zone of the Red Sea or the pull-apart basins of the southernmost Gulf of California where local patches of oceanic crust with effusive volcanism have been described.

Key words Oceanic basalts · Paleogeography · Paleotectonic evolution · Alps · Nd–Sr isotopes · Trace elements

M. Steinmann (✉)[1]
ULP-EOST-CNRS, Centre de Géochimie de la Surface, UMR 7517, 1 rue Blessig, F-67084 Strasbourg Cedex, France

P. Stille
ULP-EOST-CNRS, Centre de Géochimie de la Surface, UMR 7517, 1 rue Blessig, F-67084 Strasbourg Cedex, France

Present address:
[1]Université de Franche-Comté, Géosciences, 16 route de Gray, F-25030 Besançon Cedex, France
e-mail: marc.steinmann@univ-fcomte.fr

Introduction

Generations of geologists have tried to unravel the complex nappe pile of the present-day Alps in order to reconstruct the paleogeographic and paleotectonic evolution of the Alpine Tethys ocean during Mesozoic and Tertiary times. The presently most widely accepted lines of interpretation are outlined by three examples shown in Fig. 1.

The solutions "a" (Weissert and Bernoulli 1985) and "b" (Trümpy 1988) show the classic arrangement with the Helvetic shelf in the north, followed to the south by the North Penninic or Valais basin, the Middle Penninic or Briançonnais high, the South Penninic or Piemont-Ligurian ocean, and the continental margin of the Apulian or Adriatic plate which represented a microplate or a northern promontory of Africa. One of the main differences between the two models is the interpretation of the North Penninic realm which was the depositional site of the so-called Bündnerschiefer sediments. In solution "a" the North Penninic is interpreted as an isolated marginal basin which was completely underlain by thinned continental crust. In solution "b" the same basin is regarded as a partly oceanic basin which is replaced towards the east by the South Penninic ocean in a large-scale "en echelon" structure.

Stampfli (1993) and Stampfli and Marchant (1997) questioned the paleogeographic arrangement of solutions "a" and "b" and proposed that the Alpine Tethys initially consisted only of the South Penninic realm, and that large-scale strike-slip movements, related to the opening of the Bay of Biscay and the counter-clockwise rotation of Iberia,

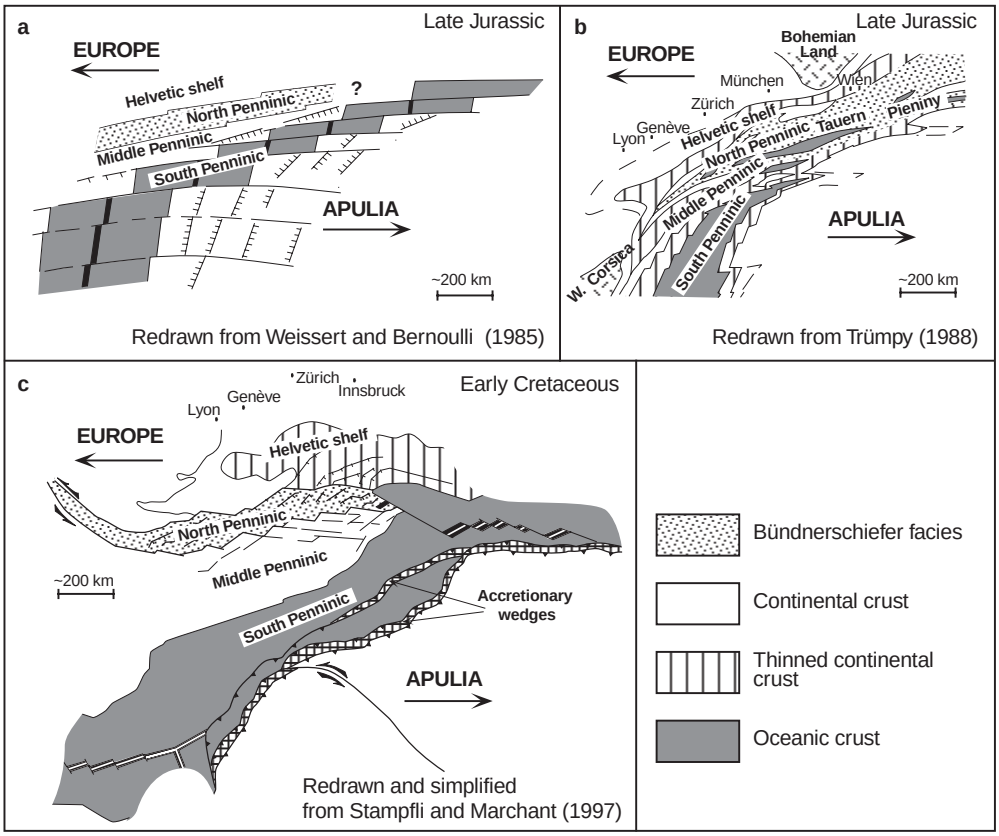

Fig. 1a–c Comparison of some paleogeographic reconstructions of the Alpine Tethys ocean. In Figs. a, b the North and South Penninic basins have reached their maximum extension, whereas in c the opening of the North Penninic basin has just started. In c the opening of the North Penninic will lead to the subduction of the South Penninic ocean and the North Penninic basin will become completely oceanic during late Early and Late Cretaceous

brought the Middle Penninic high during the Cretaceous from the west into the paleogeographic position suggested by reconstructions "a" and "b". This third interpretation is shown in Fig. 1c. It differs from the two other solutions not only by the exotic origin of the Middle Penninic High, but also by the later opening of the North Penninic basin and its subsequent complete oceanization which led to the subduction of the South Penninic ocean during the Late Cretaceous.

In contrast to the South Penninic ocean, where the existence of continuous oceanic crust is generally accepted, the interpretation of the crust beneath the North Penninic basin is different in the three reconstructions. The question as to whether it is thinned continental as in reconstruction "a", partly oceanic as in "b", or completely oceanic, as in the late stage of scenario "c", is crucial for plate tectonic reconstructions of the Alpine Tethys ocean, because the answer has direct consequences for the large-scale plate kinematic framework.

In this study we discuss the Sr and Nd isotopic and incompatible trace element composition of North Penninic basalts in order to contribute to the foregoing discussion. Our geochemical data allow not only characterization of the magma source of the basalts, but also recognition of possible chemical exchanges with subcontinental mantle or continental crust during magma ascent.

Geological context

The study area is located in the Alps of eastern Switzerland where large masses of so-called Bündnerschiefer sediments occur (Fig. 2). The term Bündnerschiefer, first introduced by Studer (1837), stands for low-grade metamorphic shaly-calcareous-terrigenous sediments deposited in the North Penninic basin. This term should not be confused with the term "schistes lustrés" used in the western Alps for lithologically similar sediments which are, in contrast to the Bündnerschiefer, of South and not of North Penninic origin.

The Bündnerschiefer units of the study area are tectonically intercalated between the Helvetic units below and the Middle Penninic, South Penninic, and Austroalpine units above. The degree of regional metamorphism is lower greenschist facies. The basaltic rocks which are the subject of the present study occur as intercalations in the so-called Misox Bündnerschiefer which represent the dominant part of the North Penninic series in the study area.

The western continuation of the Misox Bündnerschiefer is the zone of Brig-Sion-Courmayeur in the Valais (Switzerland) and in the upper Aosta Valley (Italy; Leu 1986; Trümpy 1988; Jeanbourquin and Burri 1989). This zone contains, similar to the Misox zone, metabasaltic ophiolite-like intercalations (Loubat 1968; Lasserre and Laverne 1976; Burri 1979; Cannic et al. 1997). However, the zone of Brig-Sion-Courmayeur is only narrow and tectonically

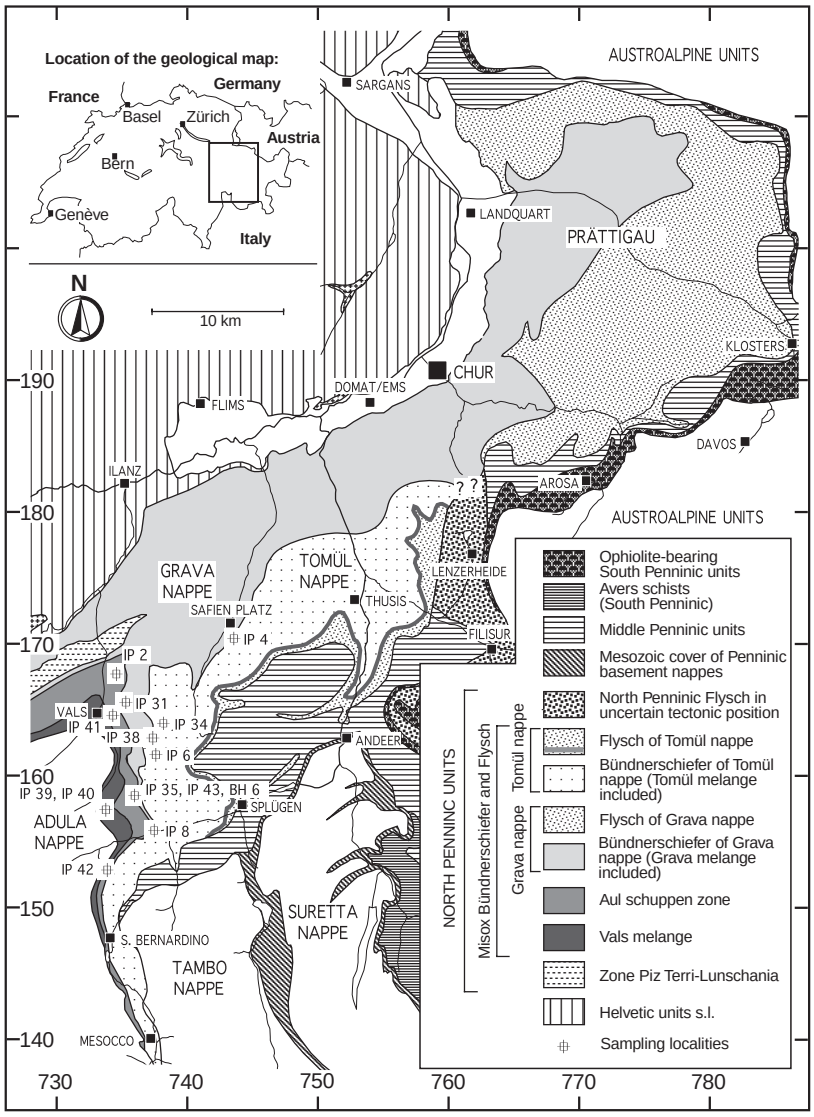

Fig. 2 Map of the study area in eastern Switzerland with sampling localities. The Tomül and Grava melanges are situated at the base of Tomül and Grava nappes and are not shown. See Table 1 for the coordinates of the sampling localities. Map from Steinmann (1994 a, b)

strongly disrupted which strongly hampers the interpretation of the data.

Towards the east, the Misox Bündnerschiefer become covered beneath Middle Penninic, South Penninic, and Austroalpine units. However, still further to the east, metabasalt-bearing Bündnerschiefer sediments reappear in the tectonic windows of Engadine and Tauern. These two occurrences are generally considered to represent the eastern prolongation of the Misox Bündnerschiefer, although they cannot directly be correlated in the field (Trümpy 1988).

A detailed description of the regional geological context of the Misox Bündnerschiefer of the study area is given by Steinmann (1994a, b) and is summarized as follows: The Misox Bündnerschiefer consists of a tectonic stack of two nappes, three melanges, and one schuppen zone. The latter ones are named Vals melange, Aul schuppen zone, Grava melange, and Tomül melange (Fig. 2) and were formed by accretion in Tertiary times. They contain sedimentary, crystalline and basaltic rocks in various proportions. A characteristic lithology among them are the Jurassic Aul marbles which dominate the Aul schuppen zone. The two nappes, called Tomül and Grava nappe, consist of an almost 2.5-km-thick pile of hemipelagic-turbiditic Bündnerschiefer sediments. These series are identical in both nappes and represent a primary sedimentary sequence covering the time interval from Late Jurassic/Early Cretaceous to Late Cretaceous. The ages of the sediments of the Aul schuppen zone and the Tomül and Grava nappes are based on lithostratigraphic comparisons and geochemical investigations (neodymium isotopes, organic carbon; Steinmann 1994a, b). In the Tomül nappe, the sediments rest with a sedimentary contact on a thick basaltic layer which forms the base of the nappe, whereas basalts are absent in the Grava nappe. The basaltic rocks discussed herein originate from the Vals and Grava melanges, the Aul schuppen zone, and from the base of the Tomül nappe.

The basalts are best preserved in the Aul schuppen zone and in the Tomül nappe. In the Aul schuppen zone, pillow

structures are observed with variolithic rims. Locally, Jurassic Aul marbles rest with a sedimentary contact upon the basalts of the Aul schuppen zone. At some places, reworked basaltic components appear in sedimentary breccias. All these observations clearly demonstrate an effusive origin of the basalts. This is in contrast to previous studies in which they were interpreted as sills (Gansser 1937; Nabholz 1945).

The basaltic layer at the base of the Tomül nappe is 30–45 m thick and can laterally almost continuously be followed over a distance of approximately 16 km. Based on field observations, this layer can be interpreted as an amalgamated sequence of submarine lava flows draped by the overlying Cretaceous Tomül Bündnerschiefer series (Steinmann 1994b). The presence of lava flows is typical for medium to high extension rates (CYAMEX 1981; MacDonald 1982). This is in contradiction to a previous study of the North Penninic basalts by Dürr et al. (1993), where based on geochemical arguments, slow extension rates have been suggested. In the other basalt-bearing units, features similar to those in the Aul schuppen zone and the Tomül nappe are observed, but the poorer preservation does not allow a clear interpretation. This is especially the case for the Vals and Grava melanges where the sediments and basalts are tectonically completely disrupted. Gabbros and serpentinites, which could represent remnants of the deeper proportions of oceanic crust, are almost entirely lacking in all North Penninic units. The only exception are the mafic and ultramafic rocks of the Chiavenna area approximately 30 km further to the south (Schmutz 1976). But their relation to the North Penninic basalts is unclear because of the complex tectonic setting. This absence of gabbros and serpentinites in the North Penninic is significantly different from the South Penninic domain where substantial amounts of such rocks are preserved.

The above-mentioned sedimentary contacts between basalts and overlying sediments allow a rough age estimate of Dogger-Malm (140–170 Ma) for the Aul basalts and Late Jurassic to Early Cretaceous (140–150 Ma) for the Tomül basalts. Despite this age difference, for simplicity we discuss the different units together and present the initial Nd and Sr isotopic compositions with a common age correction of 170 Ma.

Methods

The sampling localities are shown in Fig. 2 and listed in Table 1. TiO_2, MnO, and P_2O_5 were measured by XRF on glass beds obtained by fusion of sample powder and Li_2BO_4. Zr, Nb, Th, U, Y, and the rare earth elements (REE) were determined by ICP-MS (VG Plasmaquad PQ2+) with an analytical error less than ±5%. For the ICP-MS analyses 300 mg of sample powder were dried at 110°C, ignited at 1000°C, fused with Li_2BO_4, and then dissolved in 20 ml of a HNO_3-glycerine solution for measuring.

For Sr–Nd isotopic analysis 50 mg of sample powder were spiked with ^{87}Rb, ^{84}Sr, and ^{150}Nd–^{148}Sm tracers and subsequently dissolved in a closed Savillex vial containing 12 ml of HF 40% and 400 µl of HNO_3 65%, both of very pure quality. Digestion time was 5 days and the temperature was 150°C.

Table 1 Sample localities. Coordinates correspond to the Swiss coordinate grid

Sample	Swiss coordinates	
	Longitude	Latitude
Tomül nappe		
BH 6	737 250	160 030
IP 4	744 510	171 000
IP 6	737 730	160 630
IP 34	738 030	163 970
IP 38	737 620	163 150
IP 43	737 050	160 180
Grava melange		
IP 8	737 850	156 225
IP 31	735 900	164 650
IP 35	736 070	158 440
Aul Schuppen zone		
IP 2	734 800	167 400
IP 41	735 020	164 250
IP 42	734 810	153 000
Vals melange		
IP 39	734 050	157 220
IP 40	734 750	157 250

For Rb, Sr, and bulk REE separation 1-ml quartz columns with cation-exchange resin (AG 50W-X12, 200–400 mesh) and ammonium citrate, HCl 1.5 N, 4 N and 6 N as eluents were used. Nd and Sm were separated with the same type of resin and column and α-hydroxyisobutyric acid as eluent. The blanks at the time of analysis were <1.5 ng for Sr and <0.4 ng for Nd. Nd and Sm were measured using Ta–Re–Ta triple and Ta–Re double filament assemblies, whereas Sr was deposited on W single filaments. Sm, Nd, and Sr isotopic measurements were performed on a fully automatic VG Sector mass spectrometer with a 5-cups multicollector. The ratios $^{86}Sr/^{88}Sr=0.1194$ and $^{146}Nd/^{144}Nd=0.7219$ were used for fractionation correction. Typically, 100 ratios for Sr and Nd were collected to achieve adequate precision. The $^{85}Rb/^{87}Rb$ ratios were determined on a cameca TSN 206 single collector mass spectrometer using W filaments. The NBS 987 Sr standard solution yielded a $^{87}Sr/^{86}Sr$ value of 0.710264±10 (±stdev, n=32), and the $^{143}Nd/^{144}Nd$ ratio of the La Jolla Nd standard solution was measured at 0.511840±10 (±stdev, n=21).

The major and trace element data are compiled in Table 2, the REE data in Table 3, and the Sr and Nd isotopic data in Tables 4 and 5, respectively. Some samples have in addition been leached with 1.5 M HCl (30 min at room temperature) in order to test how much the samples had been contaminated by secondary, leachable mineral phases such as carbonates or Fe–Mn oxides. These data are compiled together with those of the unleached samples.

Table 2 Selected major and trace element data. The Y values for the Y/Nb ratios were taken from Table 3. n.d. not determined; B.D.L. below detection limit; leached sample leached with HCl 1.5 M

Sample	TiO_2	MnO	P_2O_5	Zr	Nb	Th	U	Nb/U	Nb/U (=3.2[a] Nb/Th)	Zr/Nb	Y	Y/Nb
Method[a]	1	1	1	2	2	2	2					
Tomül nappe												
BH 6	1.56	0.20	0.21	129	n.d.	n.d.	n.d.					
IP 4	1.68	0.13	0.18	130	4.4	0.91	0.14	31.2	15.4	29.7	27.88	6.38
IP 4 leached	1.91	n.d.	n.d.	128	4.1	0.60	0.23	17.7	21.9	31.4	36.17	8.84
IP 6	1.08	0.14	0.11	85	1.8	0.19	b.d.l.			47.0	24.60	13.59
IP 34	1.87	0.18	0.22	159	6.1	0.73	0.30	20.3	26.7	26.1	29.05	4.77
IP 34 leached	1.95	n.d.	n.d.	144	5.3	0.35	0.23	22.7	48.5	27.3	34.25	6.48
IP 38 leached	0.88	0.13	0.09	52	1.4	0.22	0.10	14.5	20.3	36.8	14.48	10.25
IP 43 leached	1.61	0.21	0.22	130	6.9	0.73	0.33	21.0	30.4	18.8	27.75	4.00
Grava melange												
IP 8	1.26	0.18	0.07	99	n.d.	n.d.	n.d.					
IP 8 leached	1.24	n.d.	n.d.	80	1.8	0.67	0.23	7.6	8.4	45.5	25.88	14.65
IP 31	1.02	0.14	0.11	61	3.1	0.49	0.18	17.1	20.1	19.8	37.08	12.04
IP 35	1.56	0.15	0.18	116	5.8	1.02	0.45	12.9	18.3	19.9	37.25	6.40
Aul Schuppen zone												
IP 2	1.27	0.15	0.13	82	2.3	0.20	0.07	33.0	37.0	35.5	28.77	12.46
IP 2 leached	1.49	n.d.	n.d.	87	2.4	0.30	0.11	21.8	25.2	36.3	30.24	12.66
IP 41 leached	1.26	0.14	0.14	79	3.3	0.33	0.22	15.5	32.6	23.9	26.09	7.84
IP 42 leached	1.40	0.09	0.12	90	2.9	0.28	0.29	9.9	33.3	31.3	31.41	10.92
Vals melange												
IP 39 leached	1.45	0.15	0.18	106	5.9	0.53	0.27	21.7	35.9	17.9	27.99	4.74
IP 40 leached	1.27	0.24	0.15	74	4.4	0.89	0.39	11.3	15.9	16.6	20.52	4.62

[a]1=XRF data, concentrations in percent; 2 ICP-MS data, concentrations in parts per million

Table 3 REE data (all concentrations are in ppm and analyzed by ICP-MS)

Sample	Y	La	Ce	Pr	Nd	Sm	Eu	Gd	Tb	Dy	Ho	Er	Tm	Yb	Lu	La/Sm chondrite
Tomül nappe																
IP 4	27.88	3.53	12.02	2.08	11.79	3.60	1.44	3.80	0.77	5.34	1.12	2.96	0.54	2.96	0.44	0.6
IP 4 leached	36.17	6.00	16.92	2.69	14.16	4.24	1.54	4.69	0.87	5.88	1.26	3.41	0.55	3.30	0.47	0.9
IP 6	24.60	2.92	9.36	1.64	9.38	2.96	1.24	3.28	0.69	4.76	1.03	2.66	0.50	2.68	0.41	0.6
IP 34	29.05	3.21	9.93	1.75	9.90	3.23	1.27	3.62	0.79	5.50	1.18	3.18	0.60	3.28	0.49	0.6
IP 34 leached	34.25	5.51	15.36	2.39	12.16	3.73	1.47	4.28	0.86	5.70	1.25	3.25	0.55	3.19	0.43	0.9
IP 38 leached	14.48	2.32	6.50	1.06	5.43	1.80	0.84	2.03	0.37	2.65	0.59	1.62	0.28	1.67	0.27	0.8
IP 43 leached	27.75	6.68	16.61	2.55	12.73	3.95	1.47	4.30	0.78	5.37	1.19	3.24	0.53	3.20	0.51	1.1
Grava melange																
IP 8 leached	25.88	4.21	11.21	1.66	8.36	2.59	0.99	2.92	0.58	4.17	0.94	2.42	0.40	2.38	0.36	1.0
IP 31	37.08	4.96	14.92	2.58	14.29	4.47	1.60	4.81	1.03	7.16	1.52	4.08	0.77	4.19	0.63	0.7
IP 35	37.25	6.47	18.37	3.08	16.60	5.05	1.86	5.22	1.09	7.37	1.55	4.08	0.76	4.20	0.64	0.8
Aul Schuppen zone																
IP 2	28.77	6.69	16.26	2.37	11.62	3.26	1.26	3.62	0.76	5.22	1.14	3.07	0.56	3.14	0.47	1.3
IP 2 leached	30.24	3.14	9.59	1.60	8.84	2.99	1.15	3.53	0.70	4.92	1.06	2.75	0.44	2.58	0.37	0.7
IP 41 leached	26.09	4.26	11.54	1.89	10.24	3.34	1.32	3.74	0.73	4.99	1.08	2.85	0.47	2.81	0.45	0.8
IP 42 leached	31.41	3.83	10.81	1.84	10.13	3.64	1.24	4.24	0.83	5.96	1.35	3.62	0.62	3.50	0.54	0.7
Vals melange																
IP 39 leached	27.99	6.01	15.46	2.39	12.41	3.84	1.51	4.32	0.79	5.45	1.18	3.14	0.53	2.93	0.44	1.0
IP 40 leached	20.52	5.83	13.74	1.99	9.62	2.83	1.08	3.16	0.59	4.03	0.85	2.31	0.38	2.15	0.34	1.3

Table 4 Rb–Sr isotopic data. The errors given for the $^{87}Sr/^{86}Sr$ ratios are ±2 sigma mean values and refer to the last digits. The $^{87}Sr/^{86}Sr$ (170) values are initial Sr isotopic compositions corrected for a formation age of 170 Ma

	Rb (ppm)	Sr (ppm)	$^{87}Rb/^{86}Sr$	$^{87}Sr/^{86}Sr$	$^{87}Sr/^{86}Sr$ (170)
Tomül nappe					
IP 4	4.61	181.9	0.073	0.706923(8)	0.706747
IP 4 leached	4.33	141.0	0.089	0.706933(8)	0.706718
IP 6	22.16	171.1	0.375	0.704595(8)	0.703689
IP 34	2.00	283.0	0.020	0.707554(7)	0.707506
IP 34 leached	1.66	167.6	0.029	0.707623(20)	0.707554
IP 38 leached	2.52	191.3	0.038	0.706585(11)	0.706493
IP 43 leached	6.52	148.8	0.127	0.707073(13)	0.706767
Grava melange					
IP 8	1.04	479.6	0.006	0.707689(8)	0.707674
IP 8 leached	1.01	315.1	0.009	0.707704(8)	0.707682
IP 31	18.66	389.9	0.138	0.706401(11)	0.706067
IP 35	0.77	365.3	0.006	0.704992(7)	0.704977
Aul Schuppen zone					
IP 2	0.18	191.9	0.003	0.705821(8)	0.705814
IP 2 leached	0.62	151.9	0.012	0.705646(8)	0.705617
IP 41 leached	0.96	175.8	0.016	0.705931(8)	0.705893
IP 42 leached	0.62	274.3	0.007	0.705326(10)	0.705310
Vals melange					
IP 39 leached	5.93	255.1	0.067	0.708386(9)	0.708223
IP 40 leached	8.04	372.3	0.063	0.707439(10)	0.707288

Results

The North Penninic basalts are of alkalic or tholeiitic composition (Steinmann 1994a). In ternary tectonomagmatic discrimination diagrams they plot mainly into the MORB field (Fig. 3) and their REE distribution patterns are similar to those of N-MORBs (Fig. 4). The distribution patterns of the leached samples are somewhat more enriched in the light rare earth elements (LREE, La–Nd) than the unleached ones. The chondrite normalized La/Sm ratios are ≤1.0 for most samples (Table 3). Such low values are characteristic for N-MORB but not for P-MORB, which have La/Sm chond values of 1–4 (Schilling et al. 1983). Only the samples IP 2 (unleached), IP 40, and IP 43 (both leached) have slightly higher La/Sm chond values of 1.1–1.3.

Most of the initial ε_{Nd} values of the North Penninic basalts range between +7 and +8.5 (Fig. 5). This is comparable to the composition of contemporaneous, i.e., approximately 170-Ma-old MOR basalts. Similar ε_{Nd} values have also been reported for metabasalts from the South Penninic realm (Stille et al. 1989). Only the samples IP 8 and IP 31 from the Grava melange, and IP 40 from the Vals melange, have significantly lower Nd isotopic compositions (Table 5). The initial $^{87}Sr/^{86}Sr$ ratios vary in contrast to Nd much more and range between nearly MORB-like values (0.7035) and Jurassic seawater values (0.707; Burke et al. 1982). Only sample IP 39 from the Vals melange has an Sr isotopic composition of 0.7082 which is clearly above the seawater value. The Sr and Nd isotopic compositions are in most cases not particularly different for leached and unleached samples (Tables 4, 5), indicating that the two isotope systems are not strongly affected by leachable secondary

Table 5 Sm–Nd isotopic data. The errors given for the $^{143}Nd/^{144}Nd$ ratios are ±2 sigma mean values and refer to the last digits. The ε_{Nd} (170) values are initial Nd isotopic compositions corrected for a formation age of 170 Ma and are normalized to the Chondritic Uniform Reservoir (CHUR)

	Sm (ppm)	Nd (ppm)	$^{143}Nd/^{144}Nd$	$^{143}Nd/^{144}Nd$	ε_{Nd} (170)
Tomül nappe					
IP 4	3.60	11.79	0.1846	0.512994(12)	7.21
IP 4 leached	4.24	14.16	0.1812	0.513018(4)	7.75
IP 6	2.96	9.38	0.1898	0.513049(8)	8.17
IP 34	3.23	9.90	0.1872	0.513037(11)	8.00
IP 34 leached	3.73	12.16	0.1855	0.513064(6)	8.56
IP 38 leached	1.80	5.43	0.2004	0.513028(10)	7.53
IP 43 leached	3.95	12.73	0.1877	0.513024(6)	7.73
Grava melange					
IP 8	5.40	18.73	0.1742	0.512776(14)	3.18
IP 8 leached	2.59	8.36	0.1876	0.512750(6)	2.39
IP 31	4.47	14.29	0.1794	0.512905(11)	5.59
IP 35	5.05	16.60	0.1721	0.512971(7)	7.03
Aul Schuppen zone					
IP 2	3.26	11.62	0.2031	0.513108(37)	9.04
IP 2 leached	2.99	8.84	0.2048	0.513117(4)	9.17
IP 41 leached	3.34	10.24	0.1971	0.513079(7)	8.60
IP 42 leached	3.64	10.13	0.2175	0.513124(6)	9.04
Vals melange					
IP 39 leached	3.84	12.41	0.1872	0.513047(6)	8.19
IP 40 leached	2.83	9.62	0.1782	0.512888(5)	5.28

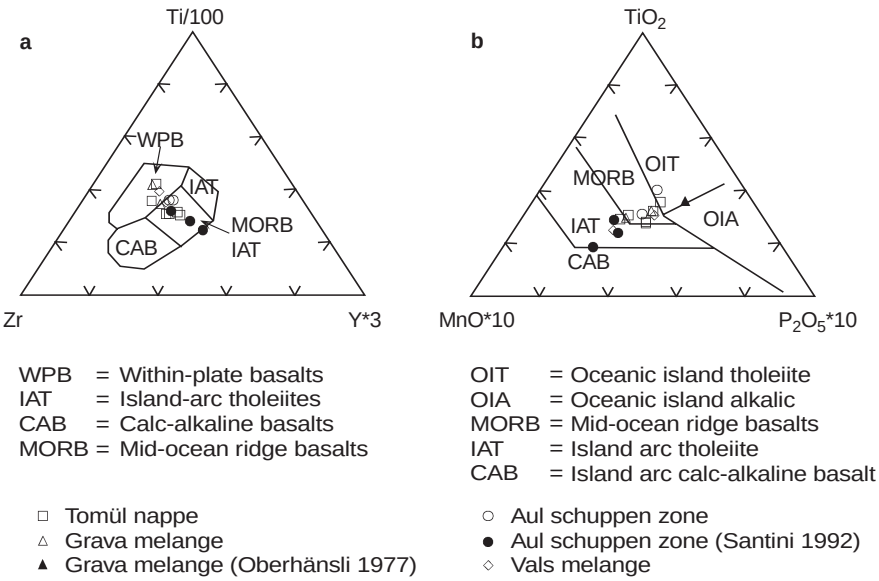

Fig. 3 Ternary discrimination diagrams for the tectonomagmatic classification of basaltic rocks after a Pearce and Cann (1973) and b Mullen (1983b). The North Penninic basalts plot mainly into the MORB field. From Steinmann (1994 a, b)

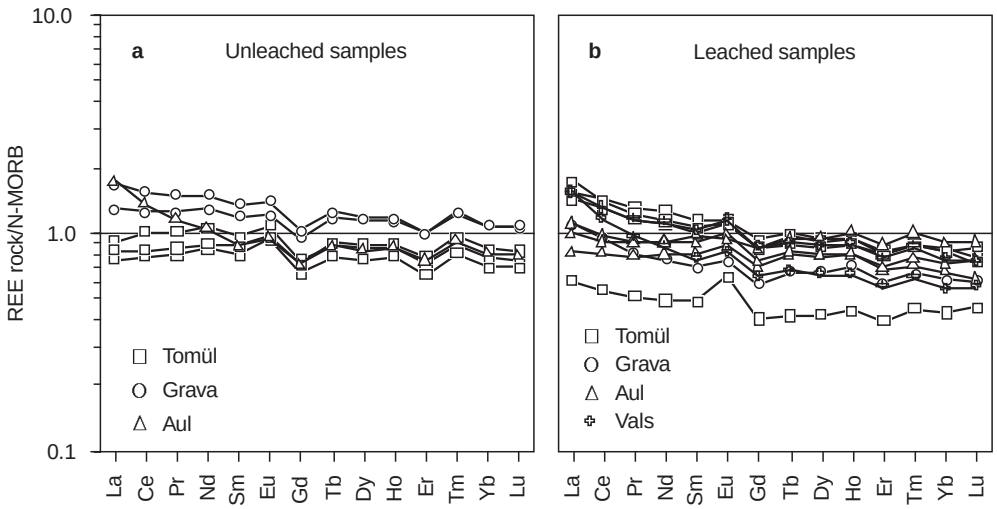

Fig. 4 REE distribution patterns of leached and unleached samples. The N-MORB values used for normalization are taken from Hofmann (1988)

mineral phases. Only sample IP 2 (Aul) shows very different Sr isotopic compositions for the leached and unleached aliquots of 0.70562 and 0.70581, respectively, whereas the ε_{Nd} values remained identical within error limits. We suggest that in this case a carbonate phase with higher $^{87}Sr/^{86}Sr$ ratios has been leached out of the sample.

In Fig. 6 the element concentration data of the North Penninic basalts were normalized to average N-MORB (Hofmann 1988) and arranged in a spiderdiagram with increasing compatibility in MORB together with the estimated composition of the bulk continental crust (Taylor and McLennan 1985). In four unleached basalt samples the most incompatible elements are shifted away from N-MORB towards more crust-like values (Fig. 6a). Only the samples IP 6 (Tomül) and IP 2 (Aul) have U and Th concentrations similar to those of N-MORB. They also have the highest Nd and lowest Sr isotopic compositions and are thus geochemically the most N-MORB-like samples. The distributions for the leached samples are basically similar as for the unleached ones, with the Aul samples being the most MORB-like (Fig. 6b).

Incompatible trace element ratios, such as Nb/U or Zr/Nb, are similar to isotope-ratio suitable tools to discriminate between different magma sources (e.g., Hofmann 1986; Hofmann et al. 1986; Hofmann 1988). In Fig. 7 the initial Nd isotopic compositions of the North Penninic basalts are plotted against their Nb/U and Zr/Nb ratios. The shown Nb/U ratios have been calculated from Nb/Th ratios using the relation Nb/U=(Nb/Th)*3.2 (Tatsumoto 1978). This is because Th can be analyzed with higher precision and is less sensitive to secondary alteration processes than U. We therefore use calculated rather than directly analyzed Nb/U ratios, although a comparison shows that there is in most cases good agreement between the two data sets (Fig. 8). The calculated ratios are generally slightly higher than the directly measured ones.

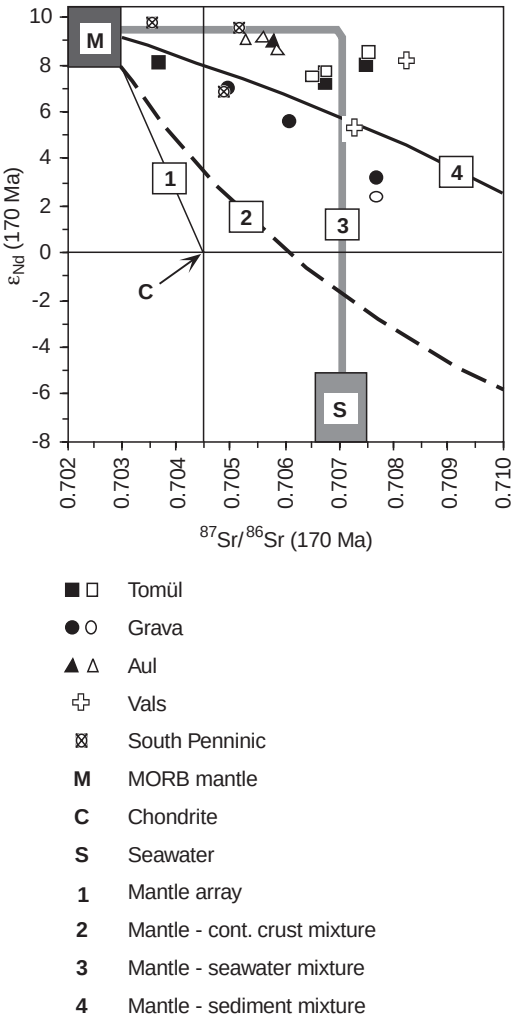

Fig. 5 Nd and Sr isotopic compositions of the North Penninic basalts. The data for the South Penninic samples are taken from Stille et al. (1989). The Sr and Nd seawater composition is from Burke et al. (1982) and Stille et al. (1996), respectively. Filled symbols unleached samples; open symbols leached samples. Curves 1–4 are calculated mixing curves, see Table 6 for end-member parameters

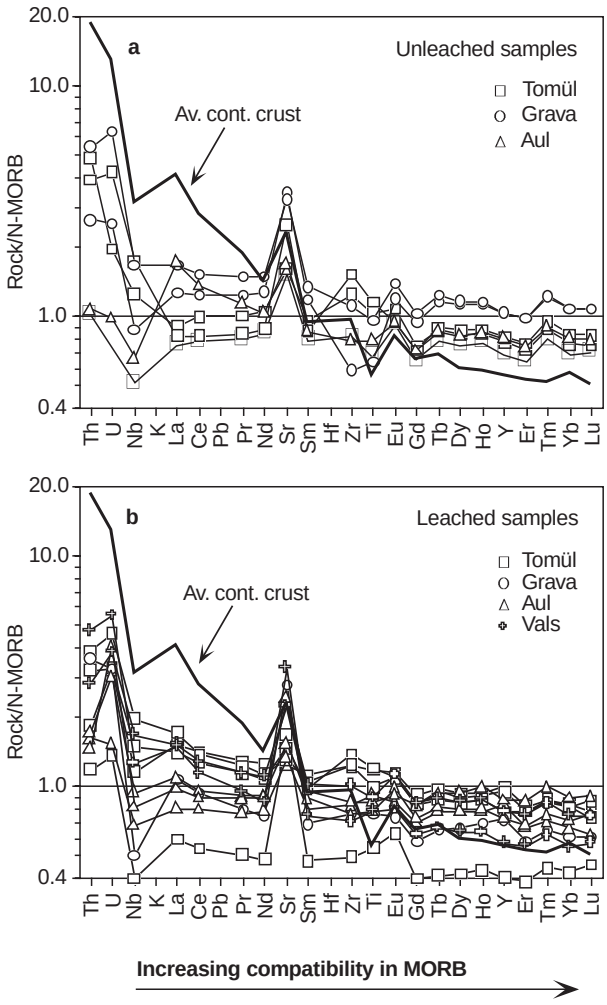

Fig. 6 N-MORB-normalized element concentrations of the North Penninic basalts plotted in the compatibility sequence of Hofmann (1988). The most incompatible elements deviate from the N-MORB composition and are shifted toward the composition of the continental crust. The N-MORB values used for normalization are from Hofmann (1988) and the composition of the average continental crust from Taylor and McLennan (1985)

Fig. 7 ε_{Nd} plotted vs the Nb/U and Zr/Nb ratios. The data points indicate a linear relation. The deviating point is in both cases sample IP 8 from the Grava melange. Filled symbols unleached samples; open symbols leached samples

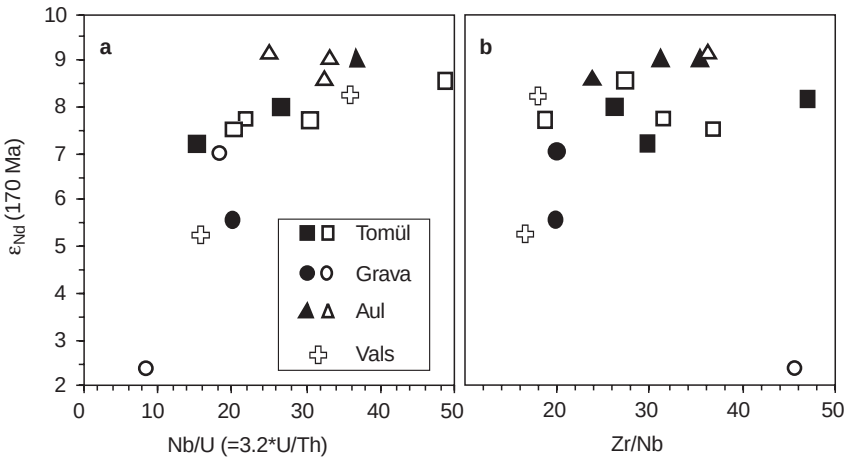

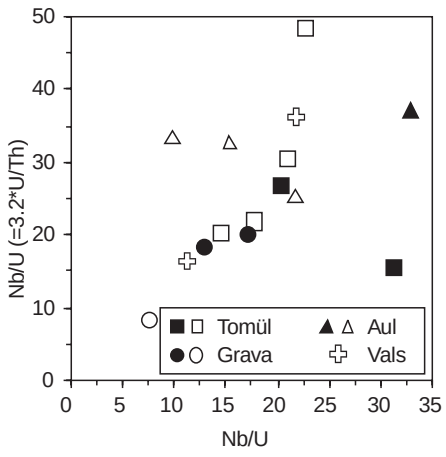

Fig. 8 The Nb/U ratios calculated from Nb/Th ratios plotted vs the measured Nb/U ratios. The calculated values are generally in good agreement with the measured ratios but always somewhat higher. Filled symbols unleached samples; open symbols leached samples

The observed Nb/U ratios range between 8 and 49. The MOR basalts have high Nb/U ratios with a global average of 47±7 (Hofmann 1986; Hofmann et al. 1986), whereas estimates for the continental crust range from 9 to 12 (Taylor and McLennan 1985). The lowest Nb/U ratios of the North Penninic basalts are thus far off from MORB values and in the range of continental crust. The Nb/U ratios are furthermore positively correlated with the Nd isotopic compositions (Fig. 7a). Samples with high ε_{Nd} values have MORB-like Nb/U ratios and the ratios get more and more crust-like with decreasing ε_{Nd}. The sample IP 8 from the Grava melange has distinctly lower Nb/U and Nd isotope ratios.

A relation similar to that of ε_{Nd} and Nb/U is also observable for the ε_{Nd} values and the Zr/Nb ratios (Fig. 7b). Typical N-MOR basalts have Zr/Nb ratios of 30 or higher (Wood et al. 1979; Hofmann 1988), whereas continental crust is characterized by values around 10 (Taylor and McLennan 1985). Almost the same crustal value has also been found for the average of 47 Bündnerschiefer sediment samples [10.1±3.2 (±stdev, *n*=47); M. Steinmann, unpublished data]. N-type MORB-like Zr/Nb ratios in the North Penninic basalts can only be observed in samples with high ε_{Nd} values. With decreasing ε_{Nd} also the Zr/Nb ratios decrease toward crustal values. Again, the sample IP 8 from the Grava melange, which already plotted off the other samples in Fig. 7a, deviates from this trend. The Zr/Nb ratios are not significantly different in the leached and unleached samples (Table 2) and are well correlated with the Y/Nb ratios (Fig. 9).

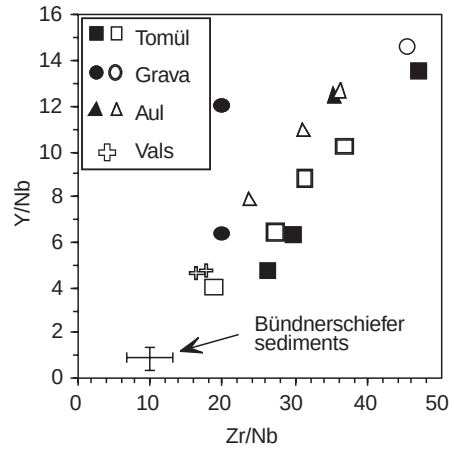

Fig. 9 Y/Nb ratios of the North Penninic basalts plotted vs their Zr/Nb ratios. The sediment value is the average of 47 Bündnerschiefer samples, the error bars are ±standard deviations. Filled symbols unleached samples; open symbols leached samples

Such covariations of Zr/Nb and Y/Nb indicate two-point mixing and can, for example, be used for the detection of crustal contamination (e.g., Dungan et al. 1986). In the North Penninic basalts the Y/Nb ratios are slightly higher in the leached than in the unleached samples. N-MOR basalts have Y/Nb ratios >8 (Wilson 1989). Decreasing ratios indicate, like decreasing Zr/Nb ratios, a crustal influence. The Y/Nb ratio of the average continental crust is 1.8 (Taylor and McLennan 1985). The average value found in the Bündnerschiefer sediments is even lower [0.9±0.5 (±stdev, *n*=47); M. Steinmann, unpublished data]. In Fig. 9 the average Zr/Nb and Y/Nb ratios of the Bündnerschiefer sediments are plotted together with the North Penninic basalts. This representation shows that an extrapolation of the linear alignment defined by the basalt samples towards lower Zr/Nb and Y/Nb ratios effectively approaches the range defined by the average Bündnerschiefer sediments.

Discussion

The REE data and particularly the chondrite-normalized La/Sm ratios point to an N-MORB origin of the North Penninic basalts. However, the isotope data and the incompatible trace element ratios suggest mixing or exchange with an additional source. In order to identify this source, we compare our Sr–Nd isotopic data with calculated mixing curves (Fig. 5). The end-member parameters used for these calculations are given in Table 6.

The covariation of the Sr and Nd isotopic compositions in Fig. 5 exclude a mixing between different mantle sources, because such a process would yield Sr–Nd isotopic

Table 6 End-member parameters used for the mixing calculations in Fig. 5

	MORB mantle	Average continental crust	Seawater	Bündnerschiefer sediments
Nd (ppm)	15	20	2.6E-06	25.5
ε_{Nd}	9.5	–12	–8	–12
Sr (ppm)	300	150	7.7	500
$^{87}Sr/^{86}Sr$	0.7025	0.718	0.707	0.718

compositions plotting on the general mantle array (trend "1" in Fig. 5). Most of the data points instead suggest a process like basalt–seawater interaction (Jacobsen and Wasserburg 1979; McCulloch et al. 1980). Alteration of basalts by seawater first leads to an increase in the $^{87}Sr/^{86}Sr$ ratios in the basalts, whereas the $^{143}Nd/^{144}Nd$ ratios remain unchanged (trend "3" in Fig. 5). This different behavior of the two isotope systems is due to, compared to Sr, the very low concentration of Nd in seawater. Only at very high water/rock ratios does also the Nd isotopic composition start to change toward seawater values.

Contamination of the basalts by continental crust, as at first view suggested by the spiderdiagrams of Fig. 6 and the covariation of ε_{Nd} with Nb/U and Zr/Nb (Fig. 7), can be excluded because the data are not in agreement with Nd–Sr mixing hyperbolas calculated with average crust and mantle parameters (trend "2" in Fig. 5). A partial fit can be obtained if the involved crustal component has a high Sr concentration, i.e., if the mixing is controlled by Sr crust-mantle concentration ratios >1.6. Such high ratios might be attained by the admixture of carbonate-rich sediments such as the Bündnerschiefer having Sr concentrations of up to 2000 ppm (M. Steinmann, unpublished data). The calculated basalt-sediment mixing curve is in good agreement particularly with the Grava samples (trend "4" in Fig. 5). The limitation of this kind of mixing to an individual tectonic unit, which furthermore is a tectonic melange zone, indicates that the exchange occurred during a tectonic rather than a magmatic process. We therefore suggest that the mixing trend observed for the Grava samples is due to fluid migration related to the formation of the Grava melange which probably took place when the North Penninic basin was subducted in the Tertiary (Steinmann 1994b; Schmid et al. 1997). A similar process could also account for the elevated Sr isotopic composition value observed for sample IP 39 from the Vals melange.

The samples from the Tomül and Aul units follow in the ε_{Nd} vs $^{87}Sr/^{86}Sr$ diagram (Fig. 5) the mixing trend no. 3 produced by basalt–seawater interaction. However, the relationship in the Y/Nb vs Zr/Nb diagram (Fig. 9) suggests that they are, despite this, also slightly contaminated by Bündnerschiefer sediments. Based on the Nd and Sr isotopic data, it can be excluded that this trend has been caused by direct contamination with continental crust.

The sediment contamination of the Tomül and Aul basalts has, in contrast to the tectonically induced sediment contamination of the Grava samples, not led to a continuous lowering of the Nd isotopic compositions and has therefore probably been caused by a different process. We suggest that it is simply due to sediment assimilation during the ascent and extrusion of the basaltic melts. Such a process could also explain the shift in the basalt samples toward crustal compositions in the spider diagram of Fig. 6 and the covariation of ε_{Nd} with Nb/U and Zr/Nb in Fig. 7. The Grava metabasalts might initially have undergone a similar contamination which was then overprinted by a second contamination during melange formation.

In any case, the data indicate that all metabasalts studied here are N-type MOR basalts which have been contaminated by sediments and seawater and which do not show a significant exchange with a more enriched mantle source or with average continental crust.

Paleotectonic implications and conclusions

The data thus show that the North Penninic basalts are directly derived from a depleted mantle source. They do not confirm the existence of subcontinental lithospheric mantle or continental crust beneath the North Penninic basin. This implies that the opening of the North Penninic realm was already so far advanced that oceanic crust could form.

The North Penninic basalts are overlain by an almost 2.5-km-thick series of siliciclastic-turbiditic Bündnerschiefer sediments. In contrast, in the South Penninic the oceanic basalts are covered by a reduced series of pelagic sediments (e.g., Weissert and Bernoulli 1985). This difference in sedimentary facies indicates that the North Penninic basin was narrower than the South Penninic ocean and suggests, together with the lack of substantial amounts of gabbros and serpentinites, that the oceanization of the North Penninic realm was not as far evolved as in the South Penninic. Modern analogues for the North Penninic basin could be the transitional zone of the Red Sea (Bonatti 1985) or the pull-apart basins of the southernmost Gulf of California (Robinson et al. 1983). In both cases, local patches of oceanic crust have been described with up to several tens of kilometers of length and width. A previous comparison of the North Penninic basin with the Gulf of California proposed by Kelts (1981) is only partly correct. This author disposed only of the field data of Nabholz (1945), where the North Penninic basalts had been interpreted as basaltic intrusions, and therefore compared the North Penninic realm with the sill-sediment complex of the central part of the Gulf of California.

The presence of local patches of oceanic crust is not compatible with solution "a" in Fig. 1 where the North Penninic basin is suggested to be completely underlain by thinned continental crust. Solution "b", in contrast, proposes a narrow basin partly underlain by oceanic crust. This is compatible with our data. Also solution "c" is in good agreement with our findings. The later opening of the North Penninic domain proposed in this latter model furthermore yields a good explanation for the Late Jurassic to Early Cretaceous age of the Tomül basalts, which are younger than the Middle Jurassic ophiolites of the South Penninic domain.

Acknowledgements Many thanks to B. Kiefel, R. Rouault, J. Samuel, and D. Tisserant for technical assistance and help provided throughout this study. The review by H.-R. Pfeifer helped to improve a previous version of the manuscript. M.S. benefited from a fellowship from the Swiss National Science Foundation, which is kindly acknowledged.

References

Bonatti E (1985) Punctiform initiation of seafloor spreading in the Red Sea during transition from a continental to an oceanic rift. Nature 316: 33–37

Burke WH, Denison RE, Hetherington EA, Koepnick RB, Nelson HF, Otto JB (1982) Variation of seawater $^{87}Sr/^{86}Sr$ throughout Phanerozoic time. Geology 10: 516–519

Burri M (1979) Les formations valaisannes dans la région de Visp. Eclogae Geol Helv 72: 789–802

Cannic S, Lapierre H, Schärer U, Mugnier JL (1997) Age, origin and geodynamic significance of the mafic-ultramafic rocks of the Versoyen complex (Valais domain, western Alps. Terra Abstr EUG 9 meeting, Strasbourg, France, March 1997, 9: 501

CYAMEX (1981) First manned submersible dives on the East Pacific Rise, 21°N. (Project RITA): general results. Mar Geophys Res. 4: 345–379

Dungan MA, Lindstrom MM, McMillan MJ, Moorbath S, Hoefs J, Haskin LA (1986) Open system magmatic evolution of the Taos plateau volcanic field, northern New Mexico. I. The petrology and geochemistry of the Servilleta basalt. J Geophys Res 91: 5999–6028

Dürr SB, Ring U, Frisch W (1993) Geochemistry and geodynamic significance of North Penninic ophiolites from the Central Alps. Schweiz Mineral Petrogr Mitt 73: 407–409

Gansser A (1937) Der Nordrand der Tambodecke. Schweiz Mineral Petrogr Mitt 17: 291–523

Hofmann AW (1986) Nb in Hawaiian magmas: constraints on source composition and evolution. Chem Geol 57: 17–30

Hofmann AW (1988) Chemical differentiation of the Earth: the relationship between mantle, continental crust, and oceanic crust. Earth Planet Sci Lett 90: 297–314

Hofmann AW, Jochum KP, Seufert M, White WM (1986) Nb and Pb in oceanic basalts: new constraints on mantle evolution. Earth Planet Sci Lett 79: 33–45

Jacobsen SB, Wasserburg GJ (1979) Nd and Sr isotopic study of the Bay of Islands ophiolite complex and the evolution of the source of mid-ocean ridge basalts. J Geophys Res 84: 7429–7445

Jeanbourquin P, Burri M (1989) La zone de Sion-Courmayeur dans la région du Simplon. Service Hydrol Géol Nat Suisse Rapports Géol 11: 1–35

Kelts K (1981) A comparison of some aspects of sedimentation and translational tectonics from the Gulf of California and the Mesozoic Tethys, northern Penninic Margin. Eclogae Geol Helv 70: 1–58

Lasserre J-L, Laverne C (1976) Le volcanisme tholéiitique de la zone du Versoyen (Alpes franco-italiennes); Minéralogie, pétrographie, et géochimie. PhD thesis, Grenoble

Leu W (1986) Lithostratigraphie und Tektonik der nordpenninischen Sedimente in der Region Bedretto-Baceno-Visp. Eclogae Geol Helv 79: 769–824

Loubat H (1968) Etude pétrographique des ophiolites de la zone du "Versoyen", Savoie (France). Arch Sci Genève 21: 265–457

MacDonald KC (1982) Mid-ocean ridges: fine scale tectonic, volcanic and hydrothermal processes within the plate boundary zone. Ann Rev Earth Planet Sci 10: 155–190

McCulloch MT, Gregory RT, Wasserburg GJ, Taylor HP (1980) A neodymium, strontium, and oxygen isotopic study of the Cretaceous Samail ophiolite and implications for the petrogenesis and seawater-hydrothermal alteration of oceanic crust. Earth Planet Sci Lett 46: 201–211

Nabholz WK (1945) Geologie der Bündnerschiefergebirge zwischen Rheinwald, Valser- und Safiental. Eclogae Geol Helv 38: 1–119

Robinson PT, Lewis BTR, Flower MFJ, Salisbury MH, Schmincke H-U (1983) Crustal accretion in the Gulf of California: an intermediate-rate spreading axis. In: Lewis BTR, Robinson P (eds) Init Rep DSDP 65. US Government Printing Office, Washington DC, pp 739–752

Schilling J-G, Zajac M, Evans R, Johnston T, White W, Devine JD, Kingsley R (1983) Petrologic and geochemical variations along the mid-Atlantic ridge from 27°N to 73°N. Am J Sci 283: 510–586

Schmid SM, Pfiffner OA, Schreurs G (1997) Rifting and collision in the Penninic zone of eastern Switzerland. In: Pfiffner OA, Lehner P, Heitzmann P, Mueller S, Steck A (eds) Deep structure of the Swiss Alps: results of NRP 20. Birkhäuser, Basel, pp 160–185

Schmutz H-U (1976) Der Mafitit-Ultramafitit-Komplex zwischen Chiavenna und Val Bondasca. Beitr Geol Karte Schweiz NF 149: 1–73

Stampfli G (1993) Le Briançonnais, terrain exotique dans les Alpes? Eclogae Geol Helv 86: 1–45

Stampfli GM, Marchant RH (1997) Geodynamic evolution of the Tethyan margins of the western Alps. In: Pfiffner OA, Lehner P, Heitzmann P, Mueller S, Steck A (eds) Deep structure of the Swiss Alps: results of NRP 20. Birkhäuser, Basel, pp 223–239

Steinmann M (1994a) Die nordpenninischen Bündnerschiefer der Zentralalpen Graubündens: Tektonik, Stratigraphie und Beckenentwicklung. PhD thesis, ETH Zürich, no. 10668

Steinmann M (1994b) Ein Beckenmodell für das Nordpenninikum der Ostschweiz. Jahrb Geol B.-A. 137/4: 675–721

Stille P, Clauer N, Abrecht J (1989) Nd isotopic composition of Jurassic Tethys seawater and the genesis of Alpine Mn-deposits: evidence from Sr–Nd isotope data. Geochim Cosmochim Acta 53: 1095–1099

Studer B (1837) Die Gebirgsmasse von Davos. N Denkschr Allgem Schweiz Ges Gesammten Naturwissen I: 1836

Tatsumoto M (1978) Isotopic composition of lead in oceanic basalts and its implication to mantle evolution. Earth Planet Sci Lett 38: 63–87

Taylor SR, McLennan SM (1985) The continental crust: its composition and evolution. Blackwell, Oxford, pp 1–312

Trümpy R (1988) A possible Jurassic-Cretaceous transform system in the Alps and the Carpathians. Geol Soc Am Spec Pap 218: 93–109

Weissert HJ, Bernoulli D (1985) A transform margin in the Mesozoic Tethys: evidence from the Swiss Alps. Geol Rundsch 74: 665–679

Wilson M (1989) Igneous petrogenesis: a global tectonic approach. Unwin Hyman, London, pp 1–466

Wood DA, Joron JL, Treuil M (1979) A re-appraisal of the use of trace elements to classify and discriminate between magma series erupted in different tectonic settings. Earth Planet Sci Lett 45: 326–336